**Validation of Ray-tracing Simulated Channels for Massive MIMO Systems at Millimeter-wave Bands**

Di , Jingyun; Yuan, Zhiqiang; Lyu, Yejian; Zhang, Fengchun; Fan, Wei

# Validation of Ray-tracing Simulated Channels for Massive MIMO Systems at Millimeter-wave Bands

Jingyun Di*, Zhiqiang Yuan‡, Yejian Lyu*, Fengchun Zhang*, and Wei Fan§¶

*Antenna, Propagation, and Millimeter-wave Systems Section, Aalborg University,
9220 Aalborg, Denmark, {dij, yely, fz}@es.aau.dk
‡Beijing University of Posts and Telecommunications, 100876 Beijing, China, yuanzhiqiang@bupt.edu.cn
§National Mobile Communications Research Laboratory, School of Information Science and Engineering,
Southeast University, Nanjing 210096, China, weifan@seu.edu.cn
¶Center for Wireless Communication-Radio Technology (CWC-RT), Oulu, Oulu University, Finland.

*Abstract*—Employing large-scale antenna configuration is seen as a key enabling radio technology for 5G and beyond communication systems. This work presents validation of a home-developed ray tracing (RT) tool for massive multiple-input multiple-output (MIMO) system in the millimeter-wave (mmWave) frequency bands. For this purpose, a channel sounding campaign in an indoor entrance scenario using a massive MIMO systems based on virtual array concept is presented. The channel measurement of 6 GHz bandwidth (26.5-32.5 GHz) is first demonstrated, with a virtual uniform circular array (UCA) consisting of 720 antenna elements located at the transmitter position on the turntable and one antenna at the receiver position. The impact of order of interactions e.g. reflections and diffractions on the channel impulse responses (CIRs) is analyzed in the RT simulation. The comparison between RT simulated and measured results shows a reasonable level of agreement.

*Index Terms*—Massive MIMO, millimeter-wave, Ray Tracing, Radio channel measurements.

## I. INTRODUCTION

Advances in fifth-generation (5G) communication systems have facilitated the development of technologies and levels of wireless communications [1] There will be more demanding requirements on the data-rate, coverage and connectivity, which necessities advancements in radio technologies. One particular technology that has garnered considerable attention within the industry and academia is massive multiple-input multiple-output (MIMO) [2]. Radio channel modeling is essential for development and performance evaluation of new radio technologies. It has been demonstrated in measurements that massive MIMO channels demonstrated several unique characteristics compared to conventional MIMO systems, including spatial non-stationary (SnS) and the presence of spherical waves [3], [4]. Therefore, the accurate characterization of radio channels, especially within the context of MIMO systems, holds paramount importance for the progression of future communications.

In millimeter-wave (mmWave) communication systems, the number of propagation paths is limited. Hence, there is a compelling case for harnessing the potential of massive MIMO technology in conjunction with mmWave communication [5]. The incorporation of massive MIMO technology enhances the energy and spectrum efficiency of the channel [6], introduces significant beamforming gains, and effectively mitigates the path loss inherent to mmWave channels [7]. Furthermore, mmWave technology inherently offers an increased bandwidth [8], and the use of shorter wavelengths enables the deployment of massive antennas with physically smaller size [3].

The practical application of massive MIMO systems has been extensive, paralleled by research into channel characterization. In the analysis of electromagnetic wave propagation, ray tracing has been a popular simulation tool. It is based on geometric optics, often involving the amalgamation of shooting and bouncing rays (SBR) along with image theory, making it a prominent choice for modeling channels in both indoor and outdoor mmWave scenarios [5], [9]. Particularly, for target sizes exceeding ten times the wavelength, RT emerges as an indispensable simulation tool in the domain of wireless communication systems [10]–[12], as it reduces the necessity for extensive measurements and allows for judicious simplifications in the scenario representation.

In this paper, the focus is to validate the home-developed ray tracing tool for the massive MIMO systems in the millimeter-wave scenarios. For this purpose the vector network analyzer (VNA)-based channel sounder proposed in [13] is employed to carry out the massive MIMO channel measurement. The experiment is performed using virtual uniform circular array (UCA), with 6 GHz bandwidth centered at 29.5 GHz [4]. We further simulate the same scenario using the ray tracing tool, and a comparative evaluation based on channel impulses responses (CIRs) from multiple positions within the virtual UCA are investigated.

The paper is organized as follows: Section II describes the measurements set up and the scenario. Section III discusses the RT simulation and the modeling of the scenario. Section IV provides a complexity analysis by comparing the results obtained through the experiments and simulations. Finally, Section V concludes the paper.

## II. CHANNEL MEASUREMENTS AND RESULTS

### A. Measurement Architecture

The measurement setup comprises a pair of vertically polarized omni-directional bi-conical antennas [14], [15], for the transmitter (Tx) and the receiver (Rx). As shown in Fig. 1, the phase-compensated VNA-based channel sounder proposed in [13] is illustrated. The operated frequency range is set to $26.5 - 32.5$ GHz, thereby providing a 6 GHz bandwidth. A total of 1800 frequency points are utilized in the frequency range, yielding a precise delay resolution of 0.167 ns and a maximum propagation distance of 90 m. The CIR corresponding to the channel frequency response (CFR) can be obtained via performing inverse Fourier transform. Utilizing a virtual UCA, the Tx contained 720 positions, and The turntable is configured to rotate 360 degrees clockwise with a 0.5 degree step, as shown in Fig. 2.
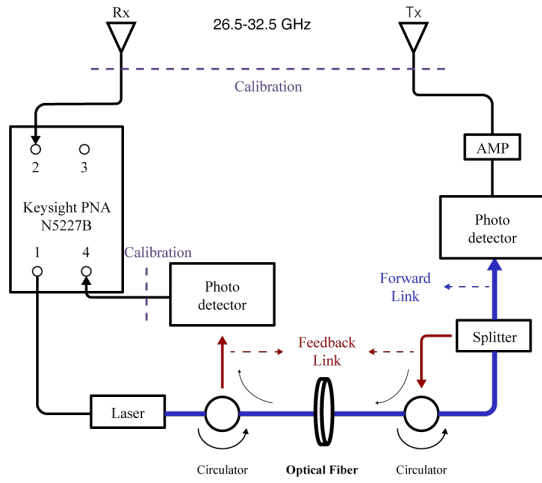


Fig. 1. Block diagrams of the VNA-based channel sounder in [13] .

### B. Channel Measurements

The measurement scenario is located on the ground floor of a building in the Aalborg University, Aalborg, Denmark. The dimensions of the enclosed room are $8.19 \times 4.78$ m$^2$, as illustrated in Fig. 2. In this scenario, several structural elements possess significance for subsequent ray tracing simulations. Notably, the room is characterized by two floor-to-ceiling glass window, an elevator, two heaters, and two wooden doors, all of which serve as critical constituents within the simulated model. Two omni-directional bi-conical antennas are used as the Tx and Rx, with the 1.25 m height of the antennas to the ground. To enable the distinction of propagation paths characterized by various time delays originating from reflections of the room's left and right boundaries, the Tx and Rx positions are strategically placed in proximity to the left wall, maintaining a separation distance of 2 meters. This configuration yields a deliberate line-of-sight (LoS) scenario, where the Tx and Rx are separated by a linear distance of 6.5 meters. For more technical details of the measurement campaign, readers are recommended to read [4].
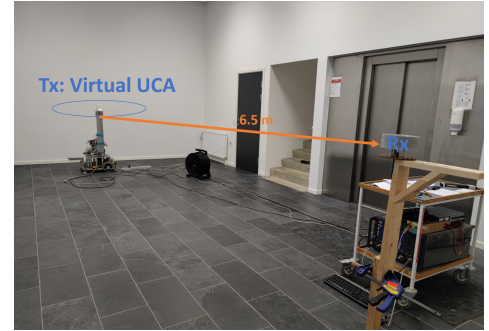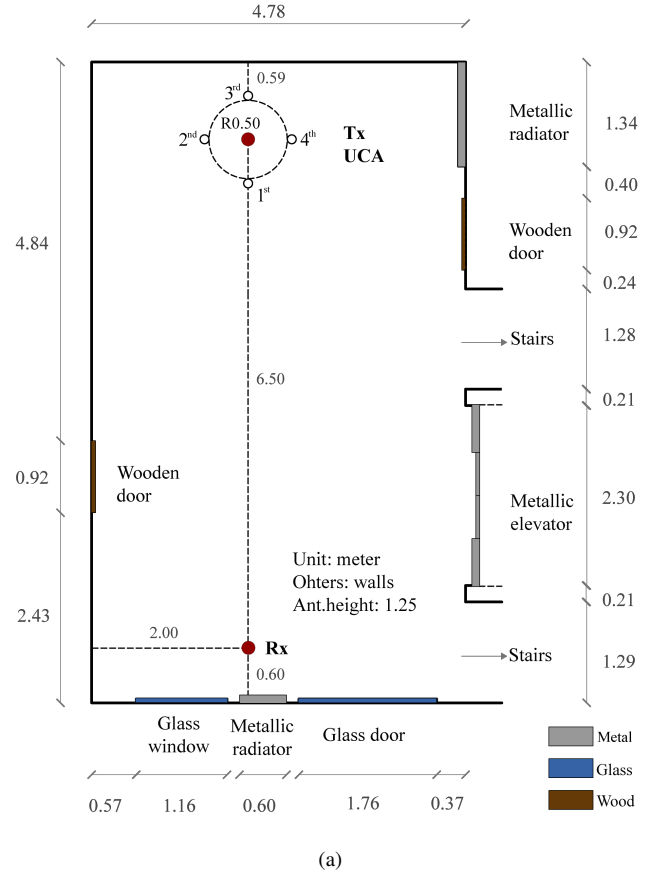


(a)



(b)

Fig. 2. (a) Measurement scenario. ((b) Photo of the indoor scenario for two antennas location.

## III. RAY TRACING SIMULATION

### A. Ray Tracing modelling

This scenario is modeled using RT tool, which is home-developed. The propagation mechanisms encompass LoS transmission, reflection, diffraction, and scattering. The vegetation model which is mainly employed for outdoor scenarios, is not considered for indoor modeling. The LoS paths in the RT are calculated based on the Friis free-space path loss equation, while reflections are calculated based on the Snell equation [16]. The diffraction is based on the uniform geometrical theory of diffraction (UTD) [17]–[19], and the scattering can be calculated based on Lambertian, Directive,

and Backscattering lobe scattering mode [20]. Consequently, the geometry of the indoor model and the parameters of the building materials assume particular significance to ensure highly accurate simulation results.

A detailed 3D model of the room, as depicted in Fig. 3, is constructed using the open-source modeling software Blender. This model includes various elements such as heating, doors, elevators, windows, etc., with their respective dimensions as labeled in Fig. 2. Material properties are concurrently assigned to these elements. The building parameters for all materials are derived from recommendations provided by the International Telecommunication Union (ITU), encompassing materials such as concrete, glass, wood, and more. The metal is defined as a perfect conductor of electricity (PEC).
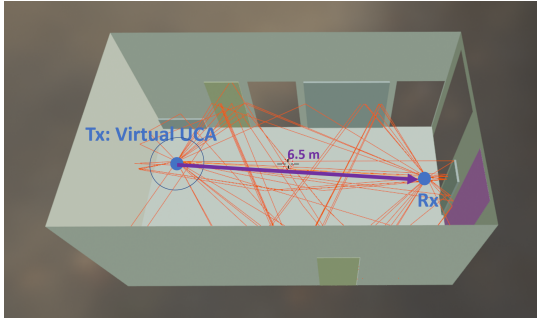


Fig. 3. RT simulation in LoS scenario.

In RT modeling, the interactions with objects can be categorized into three types: a. Reflection or diffraction mechanisms. b. Mixed modes of reflection and diffraction. c. Scattering mechanisms. Note that only the first two types of interaction with objects are considered in this work, as the focus is only on dominant propagation paths in the millimeter-wave bands. The scattering mechanism, which might be of importance for total power, etc, are not included in the following analysis.

The centering frequency used in the RT simulation is 29.5 GHz, given the coordinates of 720 antenna positions at Tx of the virtual UCA and 1 antenna position at Rx. Note that we perform simulations using one Tx-Rx position at a time. Therefore, we perform 720 simulations of these virtual antenna array (VAA) measurements. The simulation contains two step. Step 1 is for simple reflection or diffraction type, and the single simulation time is around 4 s on average. Step 2, mixed mode, for paths that have first order reflections followed by diffraction here. The single simulation time averages around 75 s. The running speed of the simulation also depends on the software environment, this RT simulation supports four parallel modules, and it takes about 4 hours to simulate the massive MIMO system, and bandwidth-limitation is in post-processing.

## IV. RESULTS COMPARISON

### A. Measurement results

As the turntable rotates, the CFRs of the 720 positions of the virtual antenna array can be recorded, with a short delay added after each measurement to ensure the stability of subsequent measurements. Fig. 4 illustrates the CIR at the first position, without the antenna gain. It is evident that the delay of the Los path is 20 ns, corresponding to a path distance of 6 m, same as the Tx-Rx distance. Both measurements and simulations exhibit a good agreement. The LoS direct path produces a deviation of less than 2 dB, potentially introduced by antenna alignment issues and inaccurate antenna gains in the datasheet.
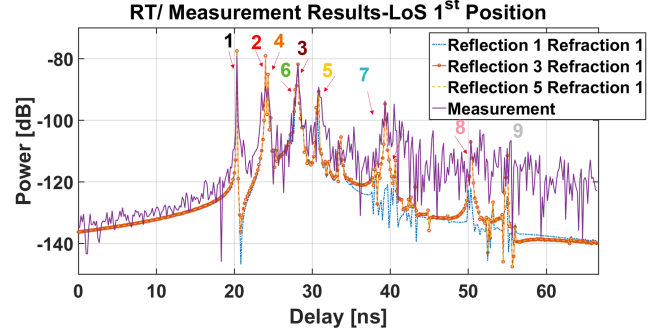


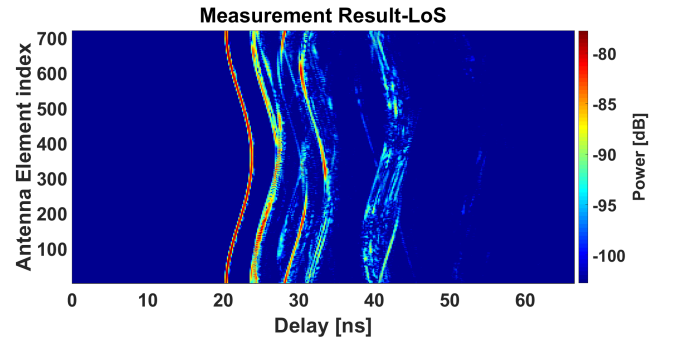Fig. 4. Comparison of different reflection order of RT and measurement results.



Fig. 5. Measured CIR in LoS scenario.

Due to the characteristics of the ultra-wideband virtual UCA, the CIR exhibits distinctive S-patterns, which facilitate the observation of dominant paths within the indoor scenario. Fig. 5 presents the CIR results across all virtual array elements for this LoS scenario, where the horizontal coordinates denote channel propagation delay, vertical coordinates indicate the antenna's position along the clockwise direction, and the color-bar represents received power, with a dynamic range of 25 dB. It is notable that the measured channel primarily concentrates within a time delay range of 20 to 40 ns. Additionally, within the mmWave band, there remains an impact attributed to scattered fields, particularly evident around a delay of 30 and 40 ns. Note that it would be neglected in the RT simulation as diffuse propagation is not considered in the simulation.

### B. Simulation results

The simulation includes the first two types of interactions with objects in the environment, with the total number of interactions capped at 3. This limit comprises a maximum of 3rd
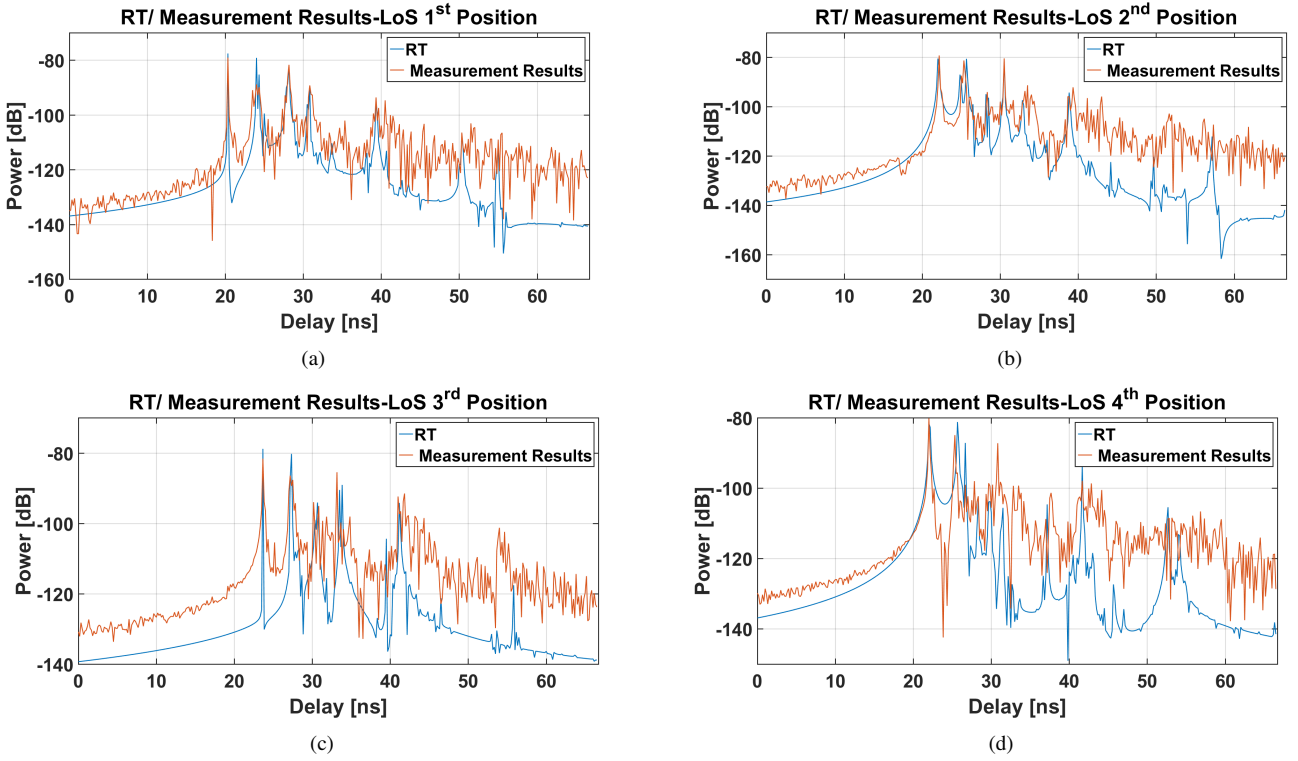
Fig. 6. CIRs at position (a) $1^{st}$ (b) $2^{nd}$ (c) $3^{rd}$ (d) $4^{th}$.
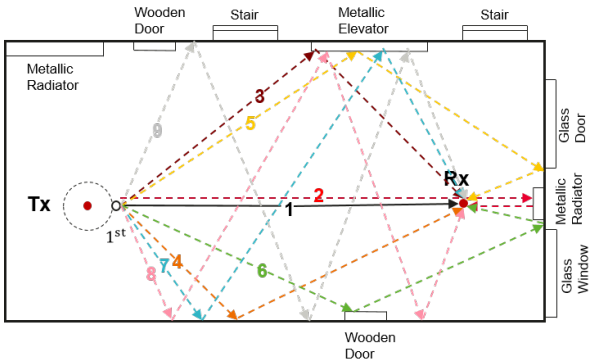


Fig. 7. Identified ray trajectory compared to room geometry.

order reflections and first order transmission. The simulation results, illustrating reflections of first, third, and fifth order, within the context of this millimeter-wave channel simulation, are visually presented in Fig. 4. Within the framework of this LoS scenario, the ray tracing simulation employs third order reflection and first order transmission to capture and analyze the primary 9 paths.

Fig. 7 depicts the path trajectories at the first antenna position, and the path analysis is derived from the RT simulation results. These results encompass electromagnetic intensity (power), delay, launch angle, arrival angle, and the polarization matrix for each path.

The CIRs are provided for four locations of the virtual array, as shown in Fig. 6. The path delays and received power levels generally align with the measurements with a reasonable agreement, though some deviations exist. In particular, position 1 and position 3 represent two points in the longitudinal direction, where the main path's delay concurs with the measurement results. However, at Position 1, there is a discrepancy of 9 dB observed at Path 2. The two positions 2 and 4 situated in the transverse direction exhibit a delay error of 0.17 ns. At position 4, the simulation still incurs an error of approximately 4 dB at Path 2. The deviations in power levels are attributable to the material parameters employed in the RT simulation, which originate from the recommendations of ITU. However, it may require adjustments to account for relative variations in building materials. Moreover, discrepancies in time delay could potentially emanate from the turntable system.

The RT simulation results for the virtual UCA are presented in Fig. 8, demonstrating a reasonable agreement with the measurement results, with a dynamic range set to 25 dB. A S-pattern comprising 9 paths becomes evident within a time delay of 80 ns. Paths 2 and 4 overlap due to their similar spatial propagation delays. The trajectories can be separately determined by analyzing the emission and arrival angles within the RT simulation results. A comparable phenomenon is observed for paths 3 and 6. However, the measurements reveal a more complex path environment, likely arising from the relatively rough surfaces of certain spatial elements. These surfaces induce stronger scattering, an aspect not considered
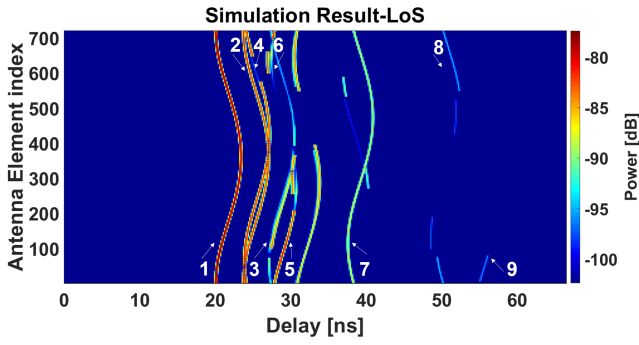
Fig. 8. Simulated CIR in LoS scenario.

in the current RT simulation.

## V. CONCLUSION

In this paper, we present a validation of ray tracing simulated millimeter-wave massive MIMO channels via comparing with practical measurements. In a LoS scenario, featuring objects such as wooden doors, elevators, and more in the environment, the measurements reveal the inherent sparsity of the millimeterwave channel. Remarkably, the measurements exhibit a reasonable agreement with the home-developed ray-tracing simulations, effectively identifying the primary propagation paths. By investigating the interaction order, specifically for this LoS scenario with third order reflections, we gain insight into the dominant propagation paths. However, within the simulation, it is noted that a few paths are absent at certain positions in the virtual UCA, which may be attributed to inaccuracies in dimensions or element placement in the model. In future work, there is still a need to optimize the building materials used in the simulations.

## ACKNOWLEDGEMENT

## REFERENCES

[1] X. Gao, L. Dai, Z. Chen, Z. Wang, and Z. Zhang, "Near-optimal beam selection for beamspace mmwave massive MIMO systems," *IEEE Communications Letters*, vol. 20, no. 5, pp. 1054–1057, 2016.

[2] E. G. Larsson, O. Edfors, F. Tufvesson, and T. L. Marzetta, "Massive MIMO for next generation wireless systems," *IEEE Communications Magazine*, vol. 52, no. 2, pp. 186–195, 2014.

[3] J. Huang, R. Feng, J. Sun, C.-X. Wang, W. Zhang, and Y. Yang, "Multi-frequency millimeter wave massive MIMO channel measurements and analysis," in *2017 IEEE International Conference on Communications (ICC)*, 2017, pp. 1–6.

[4] Z. Yuan, J. Zhang, Y. Ji, G. F. Pedersen, and W. Fan, "Spatial non-stationary near-field channel modeling and validation for massive MIMO systems," *IEEE Transactions on Antennas and Propagation*, vol. 71, no. 1, pp. 921–933, 2023.

[5] V. Degli-Esposti, F. Fuschini, E. M. Vitucci, M. Barbiroli, M. Zoli, L. Tian, X. Yin, D. A. Dupleich, R. Müller, C. Schneider, and R. S. Thomä, "Ray-tracing-based mm-wave beamforming assessment," *IEEE Access*, vol. 2, pp. 1314–1325, 2014.

[6] H. Q. Ngo, E. G. Larsson, and T. L. Marzetta, "Energy and spectral efficiency of very large multiuser MIMO systems," *IEEE Transactions on Communications*, vol. 61, no. 4, pp. 1436–1449, 2013.

[7] F. Zhang and W. Fan, "Near-field ultra-wideband mmwave channel characterization using successive cancellation beamspace UCA algorithm," *IEEE Transactions on Vehicular Technology*, vol. 68, no. 8, pp. 7248–7259, 2019.

[8] S. Huang, M. Zhang, Y. Gao, and Z. Feng, "MIMO radar aided mmwave time-varying channel estimation in MU-MIMO V2X communications," *IEEE Transactions on Wireless Communications*, vol. 20, no. 11, pp. 7581–7594, 2021.

[9] A. Karstensen, W. Fan, I. Carton, and G. F. Pedersen, "Comparison of ray tracing simulations and channel measurements at mmwave bands for indoor scenarios," in *2016 10th European Conference on Antennas and Propagation (EuCAP)*, 2016, pp. 1–5.

[10] Q. Xu and Y. Huang, *Inter-Comparison Between Antenna Radiation Efficiency Measurements Performed in an Anechoic Chamber and in a Reverberation Chamber*, 2018, pp. 305–321.

[11] K. Guan, D. He, T. Kürner, and Z. Zhong, "To know channels better: Challenges and opportunities of ray tracing," in *2023 17th European Conference on Antennas and Propagation (EuCAP)*, 2023, pp. 1–3.

[12] W. Hofmann, A. Schwind, C. Bornkessel, and M. A. Hein, "Analysis of microwave absorber scattering using ray-tracing and advanced measurement techniques," in *2022 16th European Conference on Antennas and Propagation (EuCAP)*, 2022, pp. 1–5.

[13] A. W. Mbugua, W. Fan, K. Olesen, X. Cai, and G. F. Pedersen, "Phase-compensated optical fiber-based ultrawideband channel sounder," *IEEE Trans. Microw. Theory Techn.*, vol. 68, no. 2, pp. 636–647, 2020.

[14] S. S. Zhekov, A. Tatomirescu, and G. F. Pedersen, "Antenna for ultra-wideband channel sounding," *IEEE Antennas and Wireless Propagation Letters*, vol. 16, pp. 692–695, 2017.

[15] W. Fan, I. Carton, J. Ø. Nielsen, K. Olesen, and G. F. Pedersen, "Measured wideband characteristics of indoor channels at centimetric and millimetric bands," *EURASIP Journal on Wireless Communications and Networking*, vol. 2016, no. 1, pp. 1–13, 2016.

[16] A. F. Molisch, *Wireless communications*. John Wiley & Sons, 2012, vol. 34.

[17] J. Andersen, "UTD multiple-edge transition zone diffraction," *IEEE Transactions on Antennas and Propagation*, vol. 45, no. 7, pp. 1093–1097, 1997.

[18] P. Holm, "A new heuristic UTD diffraction coefficient for nonperfectly conducting wedges," *IEEE Transactions on Antennas and Propagation*, vol. 48, no. 8, pp. 1211–1219, 2000.

[19] H. Na and T. F. Eibert, "A huygens' principle based ray tracing method for diffraction calculation," in *2022 16th European Conference on Antennas and Propagation (EuCAP)*, 2022, pp. 1–4.

[20] V. Degli-Esposti, F. Fuschini, E. M. Vitucci, and G. Falciasecca, "Measurement and modelling of scattering from buildings," *IEEE Transactions on Antennas and Propagation*, vol. 55, no. 1, pp. 143–153, 2007.